5.4. Ushuaia, Argentina (3/16/02 – 6/2/05)

This sections describes quality control of solar data recorded between 3/16/02 and 6/2/05. There were no site visits in 2003 and 2004. Solar data recorded between 3/16/02 and 12/31/03 were assigned to Volume 12; data covering the period 1/1/04 – 6/2/05 are part of Volume 14. No data were assigned to Volumes 11 and 13. Opening and closing calibrations of the 3-year period described in this section were performed on 3/15/02 – 3/17/02 and 6/3/05 – 6/4/05, respectively.

During the Volume 10 season closing site visit, which took place in the first week of January 2002, the socket of the instrument's PMT was damaged and could not be repaired. A spare socket was installed on 3/14/02. No solar data is available for the period 1/2/02 – 3/15/02 due to this problem.

The following problems affected system performance during the reporting period:

Drift of instrument responsivity
The instrument's responsivity changed by a large rate during the first half of the reporting period. This drift could be attributed to a abnormally high change of the instrument's internal irradiance lamp and changes in the throughput of the fore-optics, likely caused by abrasion from the instrument's shutter blades. The rate of change was very uniform and could be corrected without compromising the accuracy of solar data significantly.

Failure of internal reference lamp
The internal reference lamp became unstable after 10/31/03 and was replaced on 12/17/03. Between these two dates, measurements of the lamp could not be used to track the system's change in responsivity as usual, and an additional uncertainty of about 1-2% applies.

A total of 32017 scans are part of the published Ushuaia Volume 12 dataset; 26273 scans are part of Volume 14. Less than 0.3% of all scans were lost due to technical problems.

Eppley PSP and TUVR radiometers used during the periods of Volume 12 and 14 have been calibrated by Eppley Laboratory in March 2002.

5.4.1. Irradiance Calibration

The irradiance standards used in the reporting period were the lamps M-698, M-766, 200W008, and 200W026. All four lamps have also been used during the 2000/2001 season.

Lamps 200W008 and 200W026 were calibrated by Optronic Laboratories on 11/19/96 and 3/28/01, respectively. The calibration of lamp M-698 was transferred to the lamp by comparing several absolute scans from lamps M-698 and M-874, which were centered around the 1999 site visit. The method of the transfer is described in detail in Section 4.2.1.5. Lamp M-766 has an Optronic Laboratories calibration from October 1992. It was recalibrated in a similar fashion as M-698, using 1999 site visit data. The calibrations of all four site standards were the same as in the previous season. Lamp M-764 was used as traveling standard during the site visits in 2002 and 2005. It was calibrated by Optronic Laboratories on 3/28/01.

Figure 5.4.1 shows a comparison of all lamps at the beginning of the reporting period (3/15/02 – 3/17/02). All lamps agree with each other to within ±2%. Figure 5.4.2 presents a similar comparison performed at the end of the period (6/3/05 – 6/4/05). All lamps agree with each other to within ±2.5%, but the measurements of lamp 200W008 are spectrally different from the other lamps. A similar pattern, although with smaller magnitude, was already observed at the beginning of the period. In addition to lamp comparisons conducted during the site visits, lamps M-698, M-766, and 200W008 have been compared 12 times between the site visits. Lamps M-698 and M-766 typically agreed with each other to within 1-1.5%.

The agreement with lamp 200W008 was generally worse and changed significantly from calibration event to calibration event. Because of this instability, we did not use calibrations performed with lamp 200W008 for processing of solar data.

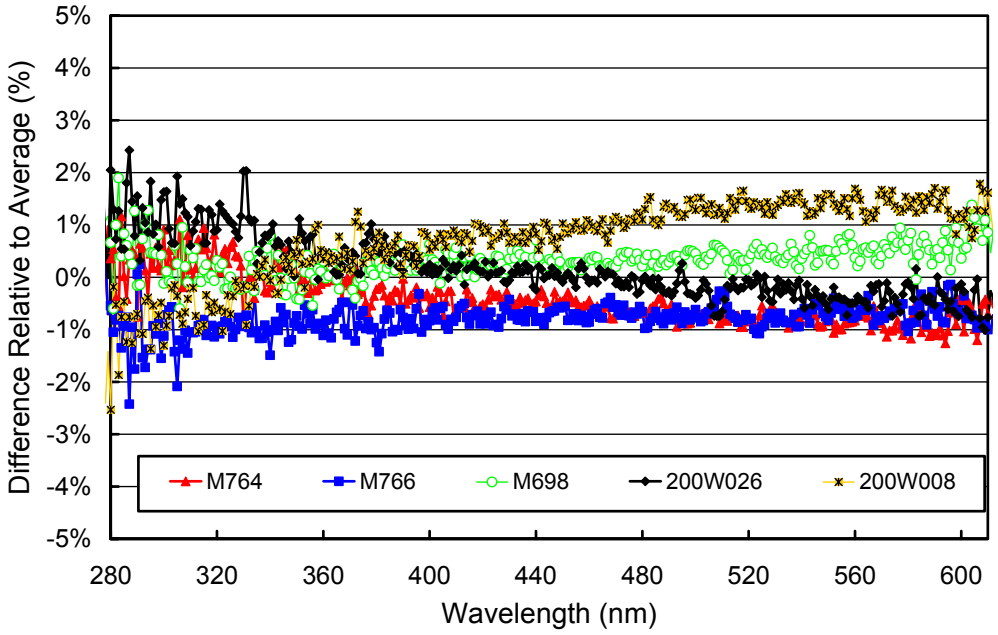

Figure 5.4.1. *Comparison of Ushuaia lamps M-698, M-766, 200W008, and 200W026, and the traveling standard M-764 at the beginning of the season (3/15/02 – 3/17/02).*

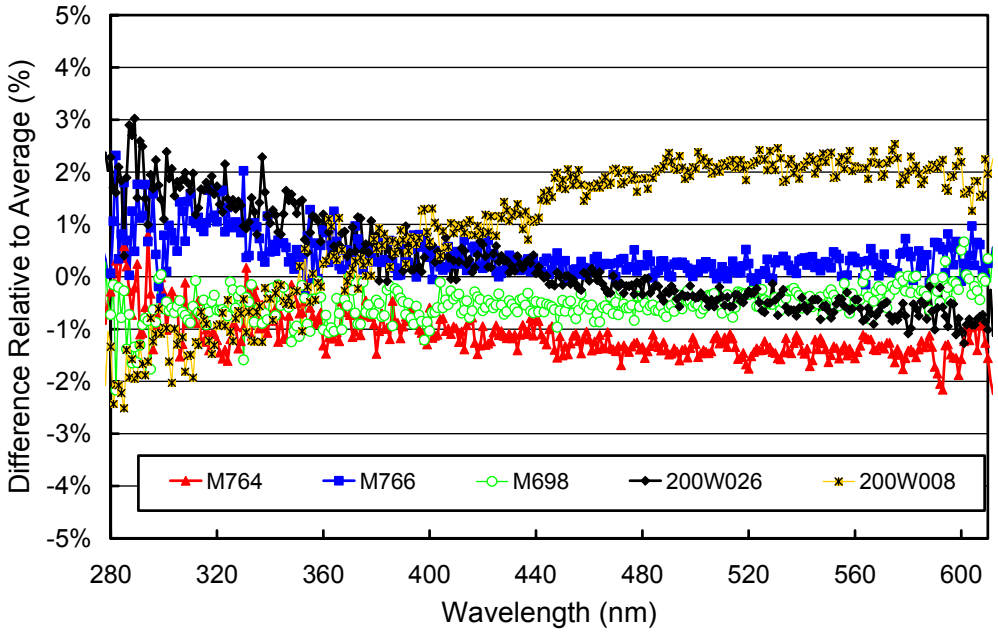

Figure 5.4.2. *Comparison of Ushuaia lamps M-698, M-766, 200W008, and 200W026, and the traveling standard M-764 at the end of the season (6/3/05 – 6/4/05).*

5.4.2. Instrument Stability

The stability of the spectroradiometer over time is primarily monitored with bi-weekly calibrations utilizing site irradiance standards and daily response scans of the internal irradiance reference. The stability of the internal lamp is monitored with the TSI sensor, which is independent of possible monochromator and PMT drifts.

By logging the PMT currents at several wavelengths during response scans, drifts in monochromator throughput and PMT sensitivity can be detected. Figure 5.4.3 shows the changes in TSI readings and PMT currents at 300 and 400 nm, derived from response scans performed between 3/15/02 and 12/17/03. Between 3/15/02 and 10/31/03, TSI measurements increased by approximately 12%, indicating a brightening of the internal lamp. PMT currents track TSI data fairly well, suggesting that monochromator throughput and PMT sensitivity remained stable to within ±3%. On 11/1/03, the lamp became unstable and was replaced on 12/17/03. Between these two dates, measurements of the lamp could not be used to track the system's change in responsivity as usual. Instead, the response scan performed on 10/22/05 was used to calibrate the system for the period 10/13/03 – 11/1/03. Likewise the response scan from 11/20/05 was used for the period 11/2/05 – 11/20/05. This procedure is acceptable since the overall system responsivity did not change during the affected period as confirmed with absolute scans using the 200-W standards.

Figure 5.4.4 shows the changes in TSI readings and PMT currents at 300 and 400 nm for the period 12/19/03 – 6/2/05. This is the period when the new lamp was installed. TSI measurements during this 1.5-year interval decreased by about 3%, indicating some dimming of the lamp. PMT currents track TSI measurements well, confirming again that monochromator and PMT were stable.

Measurements of the internal lamp cannot detect changes in the throughput of the instrument's fore optics. Absolute scans indicated that the overall responsivity of the system degraded rapidly during the first few months of the reporting period. Inspection of the instrument's optics block during the site visit in 2005 revealed that abrasion from the shutter blades had collected on the instrument's relay lens, decreasing its transmission. To correct for the loss in sensitivity, the instrument's calibration was broken into 26 periods, which are summarized in Table 5.4.1.

Figure 5.4.5 presents ratios of irradiance spectra applied to the internal lamp during periods P1B – P12, referenced to the spectrum for Period 1. The figure shows that the spectra changed by about 40% in the UV-B and 20-25% in the visible. The change is very monotonous over time, allowing to correct the drift with little uncertainty. Figure 5.4.6. shows ratios of irradiance spectra applied to the internal lamp during Periods P14 – P17, referenced to the spectrum for Period P13. Changes are smaller than ±5%.

As explained in Section 4.2.1.2, the irradiance assigned to the internal lamp in each period is the average of individual spectra determined from absolute scans measured in that period. The standard deviation of the individual spectra allows estimating the variability of the calibrations in each period. Figure 5.4.7 shows that the standard deviation in the UVA and visible is less than 1.5% of the average for all periods, with the exception of Period P13 where it is slightly higher. This confirms the good consistency of absolute scans for all assigned periods.

Table 5.4.1 Calibration periods for Ushuaia Volumes 12 and 14.

Period name	Period range	Volume	Number of Absolute scans	Remarks
P1	01/07/02 - 03/18/02	12	8	
P1B	03/19/02 - 03/25/02	12	0	Interpolated from P1, P2
P2	03/26/02 - 04/20/02	12	3	
P3	04/21/02 - 05/01/02	12	1	
P3B	05/02/02 - 05/14/02	12	0	Interpolated from P3, P4
P4	05/15/02 - 06/10/02	12	2	
P4B	06/11/02 - 06/23/02	12	0	Interpolated from P4, P5
P5	06/24/02 - 07/04/02	12	4	
P5B	07/05/02 - 07/17/02	12	0	Interpolated from P5, P6
P6	07/18/02 - 08/13/02	12	1	
P6B	08/14/02 - 08/27/02	12	0	Interpolated from P6, P7
P7	08/28/02 - 09/24/02	12	5	
P7B	09/25/02 - 09/30/02	12	0	Interpolated from P7, P8
P8	10/01/02 - 12/20/02	12	5	
P8B	12/21/02 - 12/31/02	12	0	Interpolated from P8, P9
P9	01/01/03 - 03/13/03	12	3	
P10	03/14/03 - 04/09/03	12	3	
P10B	04/10/03 - 05/07/03	12	0	Interpolated from P10, P11
P11	05/08/03 - 09/10/03	12	10	
P11B	09/11/03 - 12/04/03	12	0	Interpolated from P11, P12
P12	12/05/03 - 12/17/03	12	3	
P13	12/18/03 - 03/11/04	12 and 14	3	
P14	03/12/04 - 09/01/04	14	12	
P15	09/02/04 - 11/17/04	14	4	
P16	11/18/04 - 05/21/05	14	10	
P17	05/22/05 - 06/05/05	14	8	

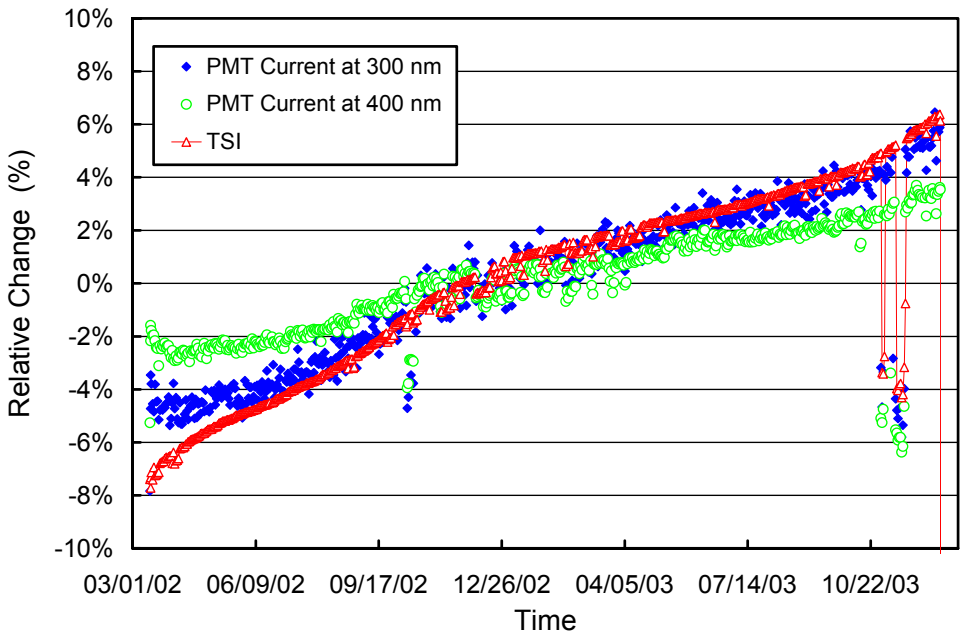

Figure 5.4.3. *Time-series of TSI signal and PMT currents at 300 and 400 nm during measurements of the internal reference lamp performed at Ushuaia between 3/15/02 and 12/17/03. After 10/31/03, the internal lamp became unstable and was replaced on 12/17/03. Between these two dates, measurements of the lamp could not be used to track the system's change in responsivity as usual.*

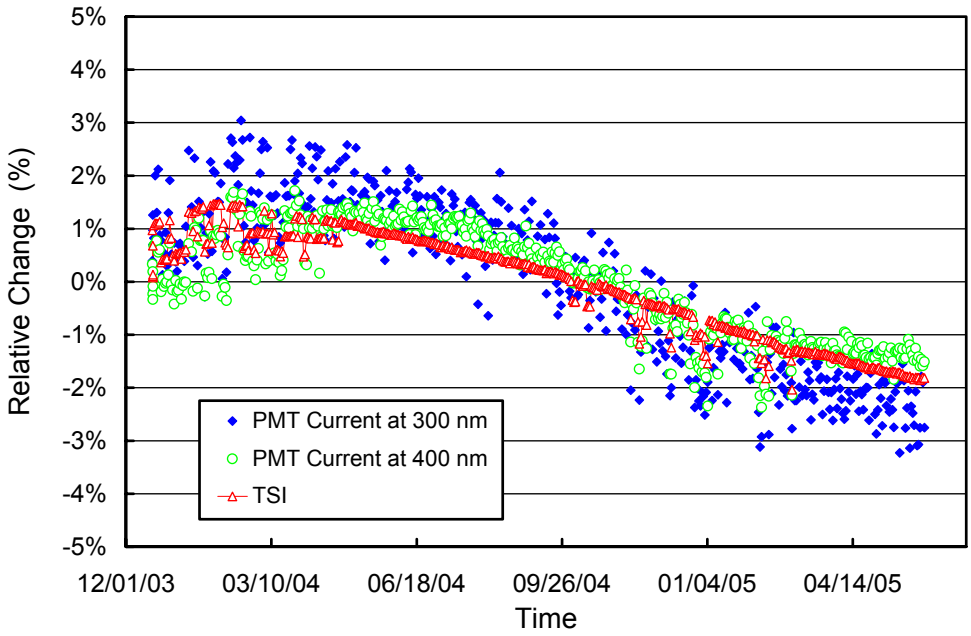

Figure 5.4.4. *Time-series of TSI signal and PMT currents at 300 and 400 nm during measurements of the internal reference lamp performed at Ushuaia between 12/19/03 and 6/2/05. This is the period when the second internal lamp was installed.*

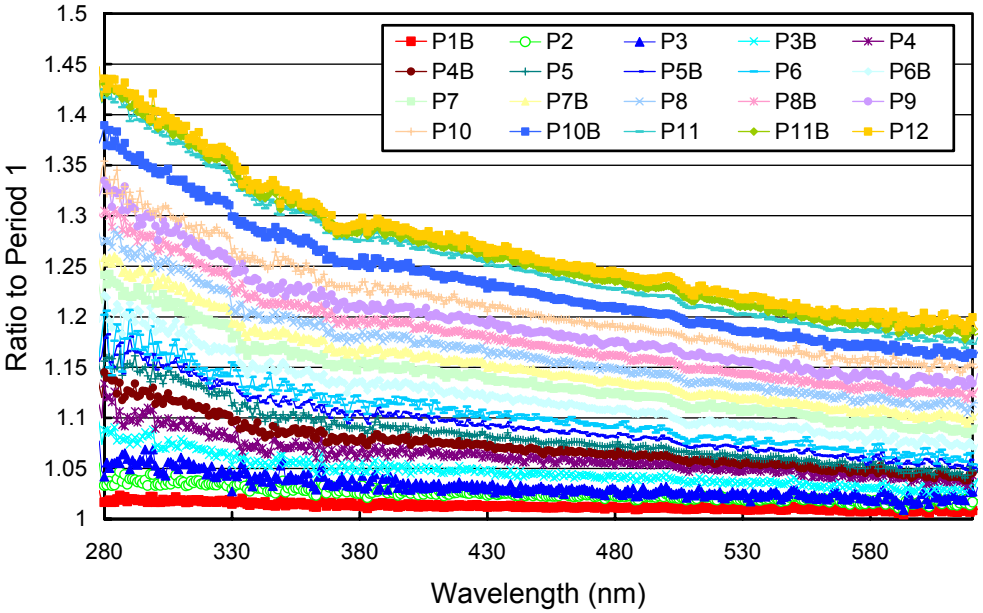

Figure 5.4.5. *Ratios of irradiance assigned to the internal reference lamp in Periods P1B - P12, referenced to the irradiance of Period P1.*

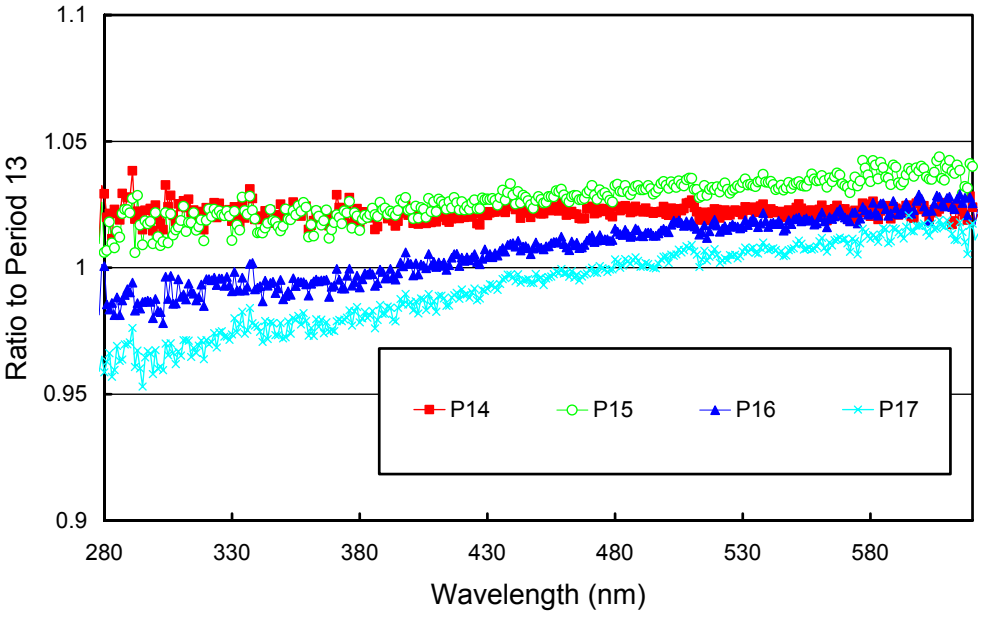

Figure 5.4.6 *Ratios of irradiance assigned to the internal reference lamp in Periods P14 - P17, referenced to the irradiance of Period P13.*

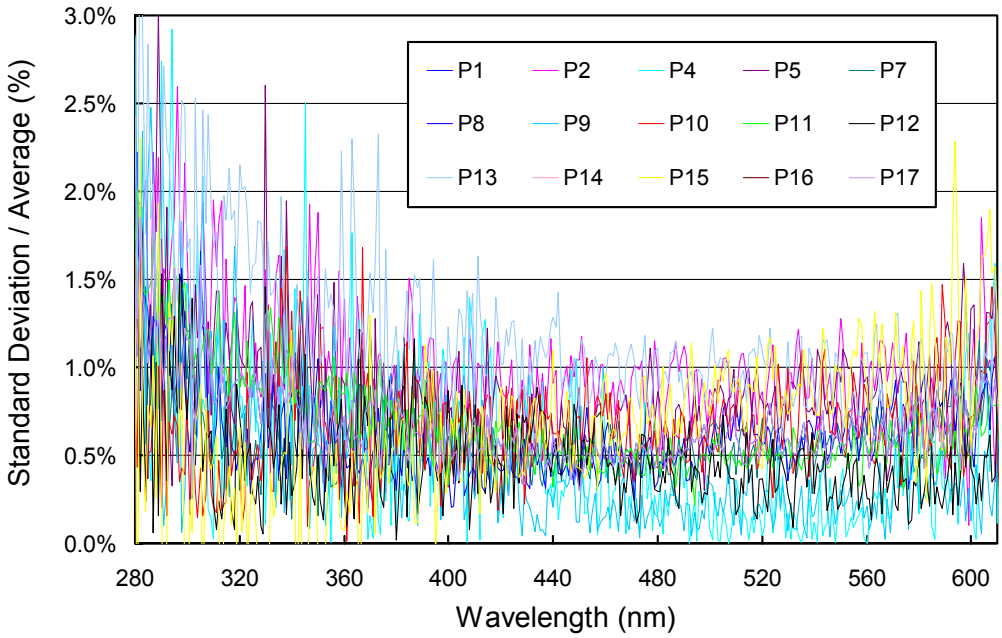

Figure 5.4.7. *Ratio of standard deviation and average calculated from the absolute calibration scans measured at Ushuaia between 3/15/02 and 6/4/05.*

5.4.3. Wavelength Calibration

Wavelength stability of the system was monitored with the internal mercury lamp. Figure 5.4.8 shows the differences in the wavelength offset of the 296.73 nm mercury line between pairs of consecutive wavelength scans for the period 3/16/02 – 12/31/03. In total, 658 scans were evaluated. For 99.5% of the scans is the difference in the wavelength offset to neighboring scans less than ±0.055 nm. Figure 5.4.9 shows a similar plot for the period 1/1/04 – 6/2/05. 516 scans were evaluated. For 98.8% of the scans is the difference in the wavelength offset to neighboring scans less than ±0.055 nm. Changes larger than ±0.1 nm were caused by instrument problems or operator intervention. Affected data were adjusted accordingly.

After the data was corrected for day-to-day wavelength fluctuations, the wavelength-dependent bias between this homogenized data set and the correct wavelength scale was determined with the Fraunhofer-line correlation method (Chapter 4). For the Volume 12 period, four correction functions were established and are shown in Figure 5.4.10. The correction function for the Volume 14 period is plotted in Figure 5.4.11.

After the data was corrected using the shift function described above, the wavelength accuracy was verified with the Fraunhofer method. The results for noon-time spectra are shown for four UV wavelengths in Figure 5.4.12 (Volume 12 period) and Figure 5.4.13 (Volume 14 period). Residual shifts are typical smaller than ±0.05 nm. Few outliers occur when spectra are distorted due to changing cloud cover. The wavelength stability is not worse during cloudy conditions but the validation is subject to larger uncertainties.

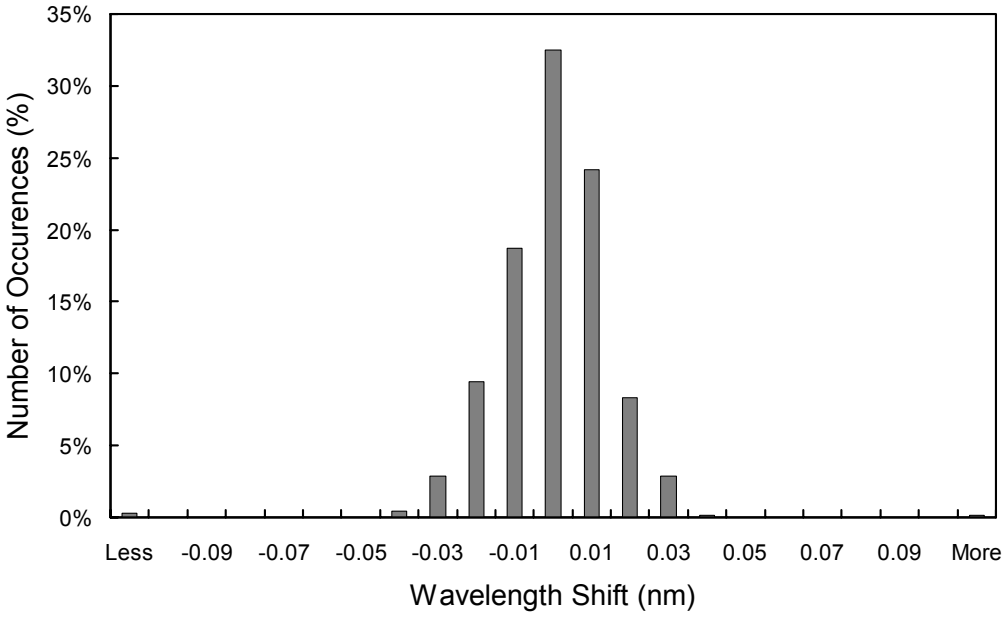

Figure 5.4.8. *Differences in the measured position of the 296.73 nm mercury line between consecutive wavelength scans for the period 3/16/02 – 12/31/03. . The labels of the horizontal axis give the center wavelength shift for each column. The 0-nm histogram column covers the range from -0.005 to +0.005 nm. "Less" means shifts smaller than -0.105 nm; "more" means shifts larger than 0.105 nm.*

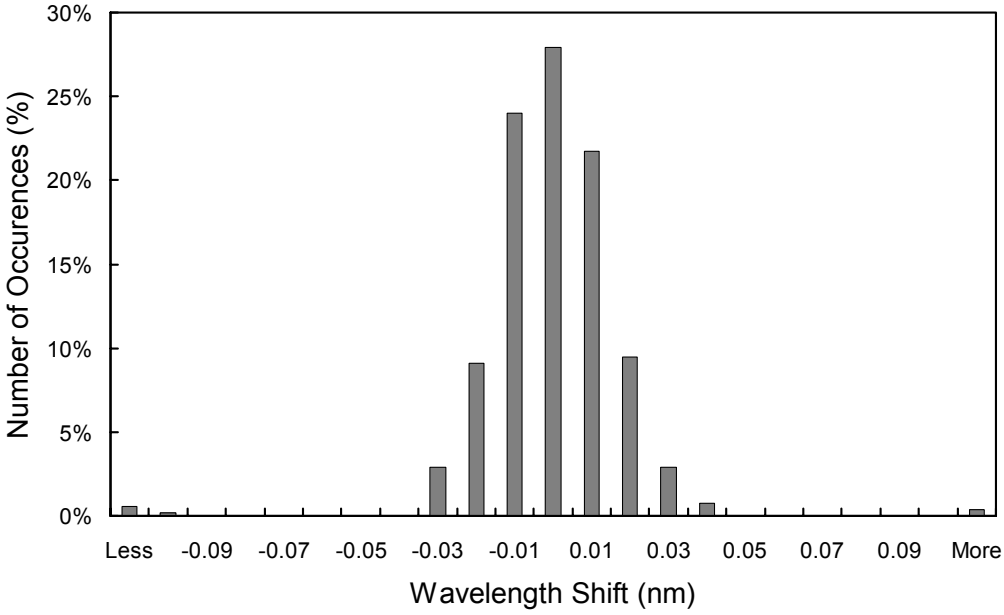

Figure 5.4.9. *Same as figure 5.4.8 but for the period 1/1/04 – 6/2/05.*

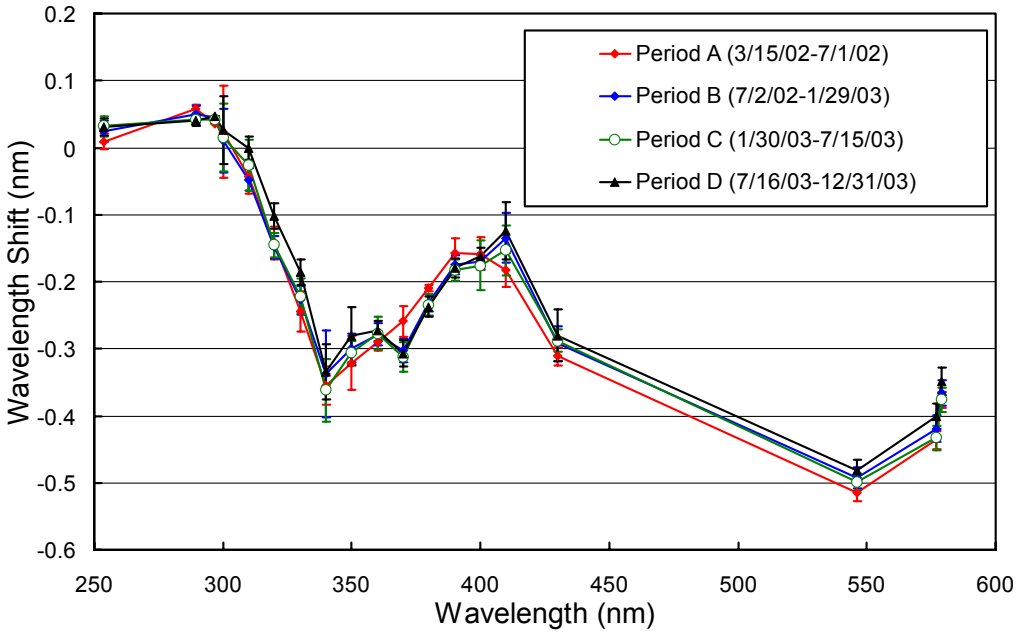

Figure 5.4.10. *Monochromator non-linearity correction functions for the Volume 12 period at Ushuaia. The error bars are the 1σ standard deviation of the wavelength shift for the periods indicated in the legend.*

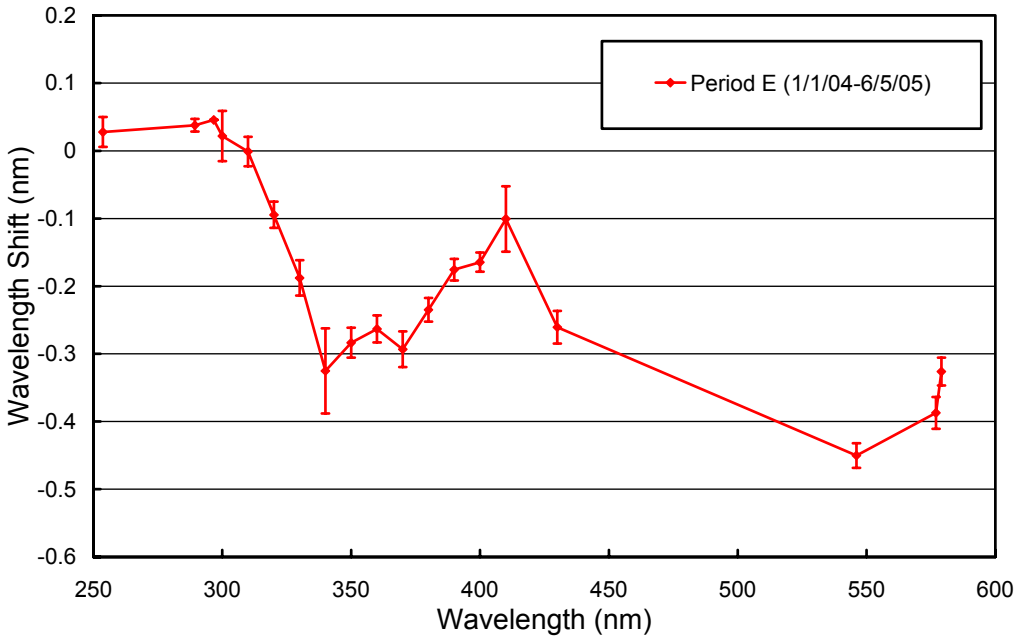

Figure 5.4.11. *Monochromator non-linearity correction functions for the Volume 14 period at Ushuaia. The error bars are the 1σ standard deviation of the wavelength shift for the periods indicated in the legend.*

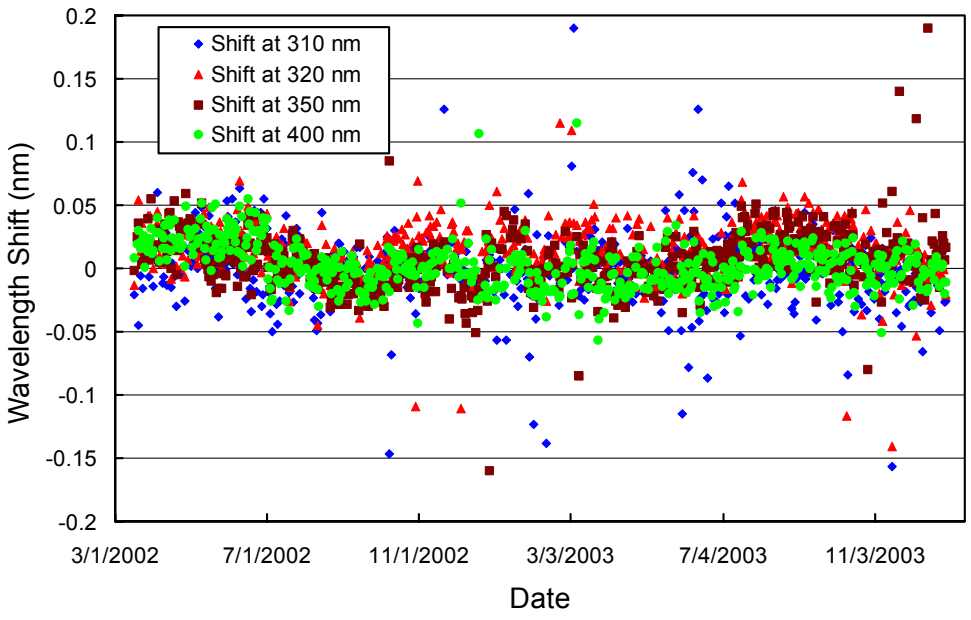

Figure 5.4.12. *Wavelength accuracy check of final data at four wavelengths in the UV by means of Fraunhofer-line correlation. The noontime measurement has been evaluated for each day of the Volume 12 period.*

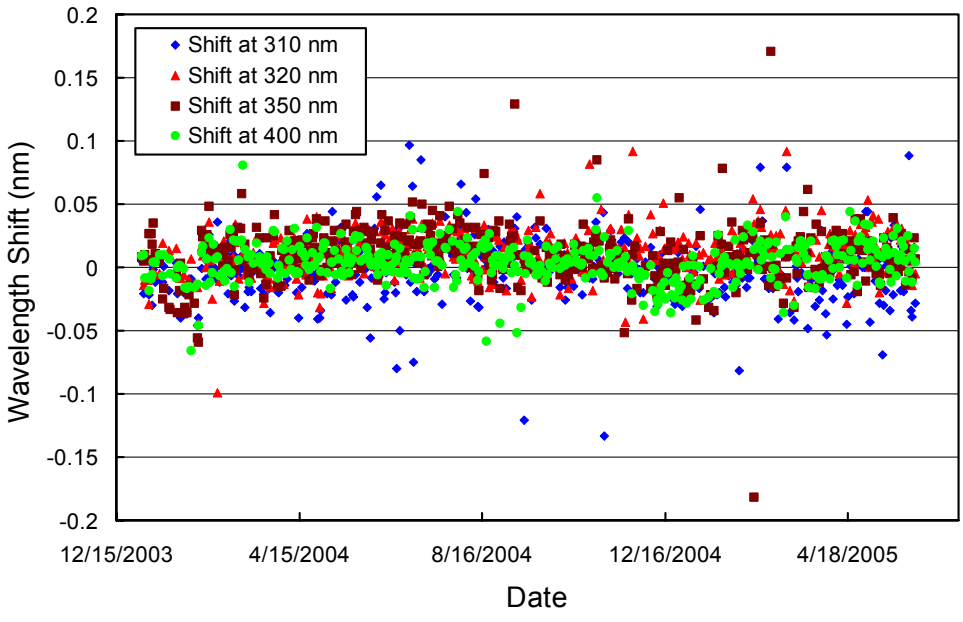

Figure 5.4.13. *Wavelength accuracy check of final data at four wavelengths in the UV by means of Fraunhofer-line correlation. The noontime measurement has been evaluated for each day of the Volume 14 period.*

Although data from the external mercury scans do not have a direct influence on the data products, they are an important part of instrument characterization. Figure 5.4.14 illustrates the difference between internal and external mercury scans collected during the season closing site visit. Data from the opening visit are not available. The wavelength scale of the figure is the same as applied during solar measurements. The peak of the external scans agrees approximately with the nominal wavelength of 296.73 nm, whereas the peak of the internal scans is shifted by about 0.12 nm to shorter wavelengths. External scans have a bandwidth of about 1.00 nm FWHM; the bandwidth of the internal scan is 0.70 nm. External scans have the same light path as solar measurements and represent the monochromator's bandpass relevant to solar scans.

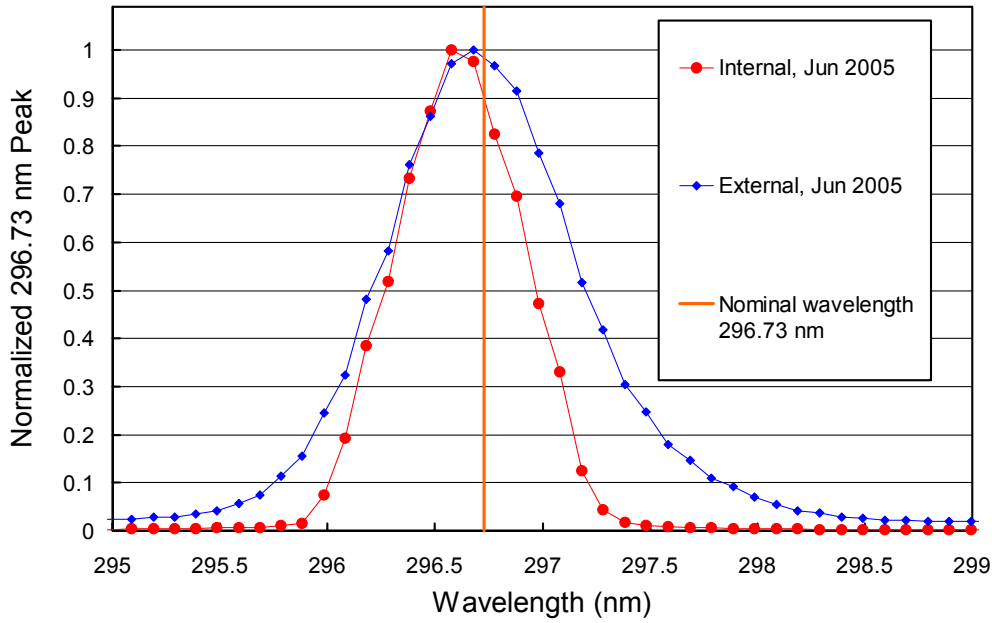

Figure 5.4.14. *The 296.73 mercury line as registered by the PMT from external and internal sources. The wavelength scale is the same as applied for solar measurements, i.e., it is based on a combination of internal scans and the Fraunhofer-correlation method. It is assumed that the wavelength registration of the monochromator did not shift between internal and external scans, which were close in time.*

5.4.4. Missing Data

Volume 12 (3/16/02 – 12/31/03):
A total of 32017 solar scans are part of the published Ushuaia Volume 12 dataset. These are 98% of all possible solar scans. Only 0.3% of all scans were missed due to technical problems. Of all additional missing scans, 378 were superseded by absolute, 19 by response and 9 by wavelength scans. 12 scans were lost on 9/6/03 due to a full hard drive. 74 scans were lost on 12/3/03 when the GPS receiver erroneously reset the time by one day.

Volume 14 (1/1/04 – 6/2/05):
A total of 26273 solar scans are part of the published Ushuaia Volume 14 dataset. These are 98% of all possible solar scans. Less than 0.2% of all scans were missed due to technical problems. Of all additional missing scans, 251 were superseded by absolute, 4 by response and 7 by wavelength scans. 21 scans were lost on 2/9/04 and 2/10/04 due to communication problems between computer and control hardware (spectralink). For a similar reason, 13 scans were lost on 3/1/05 and 3/2/05.